Proceedings of the Twenty-seventh (2017) International Ocean and Polar Engineering Conference **www.isope.org**
San Francisco, CA, USA, June 25-30, 2017

ISBN 978-1-880653-97-5; ISSN 1098-6189

Effects of the Arrangement of Vertical Baffles on Liquid Sloshing by MPS Method

*Xiang Chen, Youlin Zhang, Decheng Wan**
Collaborative Innovation Center for Advanced Ship and Deep-Sea Exploration, State Key Laboratory of Ocean Engineering, School of Naval Architecture, Ocean and Civil Engineering, Shanghai Jiao Tong University, Shanghai, China
*Corresponding author

ABSTRACT

This paper presents a numerical analysis of liquid sloshing in a rectangular tank under translational excitation. The numerical tool used in this study is an in-house solver MLParticle-SJTU which is developed based on improved moving particle semi-implicit (MPS) method. The validity of solver is proved by comparing the results of numerical simulation and experiment in three-dimensional (3-D) tank without baffles. The impact pressure on lateral wall and the deformation of free surface are investigated. In order to reduce sloshing amplitude, vertical baffles are installed in the middle of tank. Furthermore, the arrangement of vertical baffles is changed to research the effects on impact pressure and fluid field. The comparison of numerical results shows that the arrangement of vertical baffles plays an important role in impact pressure and fluid field.

KEY WORDS: MPS; MLParticle-SJTU solver; liquid sloshing; vertical baffles.

INTRODUCTION

The motion of fluid in a partially filled tank is called as sloshing, which is a physical phenomenon characterized by the oscillation of the unrestrained free surface. With the demand of energy increasing, many vessels that transport liquefied natural gas and oil have been constructed such as LNG, FPSO and FLNG. Sloshing is induced in liquid cargo tank by the movement of the vessels. It poses a great threat to the ship security and structural strength of tank. Therefore, many researchers have devoted themselves to investigating the characters and mechanisms of sloshing which is a complex nonlinear problem.

Faltinsen (1978) developed a linear analytical solution for 2-D liquid sloshing in a rectangular tank under horizontal excitation. Then, Nakayama and Washizu (1980) used the finite element method (FEM) to study 2-D problem of non-linear liquid sloshing in a rectangular tank under pitch excitation. And they (1981) used the boundary element method (BEM) to analyze 2-D non-linear liquid sloshing. Wu et al. (1998) employed FEM to simulate the 3-D liquid sloshing in the tank. Koh et al. (1998) developed a coupled BEM-FEM to investigate 3-D liquid sloshing in rectangular tank. Based on the Bateman-Luke variational principle, Faltinsen et al. (2000) derived the multidimensional modal system to describe nonlinear sloshing and verified the validness of this theory by experiments. Liu and Lin (2008) developed a numerical model to study 2-D and 3-D viscous and inviscid liquid sloshing in rectangular tanks by using the second-order accurate volume-of-fluid (VOF) method to track the distorted and broken free surface. Now, many Lagrangian particle methods are also used to study sloshing problems. Shao et al. (2012) applied one mesh-free method, smoothed particle hydrodynamics (SPH), to simulate 2-D liquid sloshing. Yang et al. (2015) studied the effects of excitation period on 2-D Liquid Sloshing by MPS Method. With the development of equipments, the experiments gradually catch up with the theoretical and numerical researches. Delorme et al. (2009) carried out a series of experiments to research the impact pressure of sloshing in shallow filled tank under roll excitation. Xue et al. (2013) conducted a series of laboratory experiments to study the sloshing of a two-liquid system in a rectangular tank by changing external excitation frequency. Bulian et al. (2014) focused on the analysis of impact pressure registrations from repeated model scale sloshing experiments under harmonic rotational excitation. Souto-Iglesias et al. (2015) studied the influence of tank width on impact pressure statistics in regular forced angular motion by experimental research. Park et al. (2015) modified the shape of LNG tank and conducted experimental tests to validate the effectiveness of the modified tank with different filling depths.

Through extensive research works, the characters and mechanisms of sloshing are gradually mastered by researchers. The method to reduce sloshing impact pressure and restrain the deformation of free surface has been novel focus. At first, the effect of a single vertical baffle on reducing sloshing is investigated. Arai et al. (1992) used the Marker-and-cell (MAC) method to simulate numerically a 3-D sloshing phenomenon in liquid tank with vertical baffle by comparing it with experiment. Liu and Lin (2009) modeled the vertical baffle in 2-D and 3-D tank by virtual boundary force (VBF) method. Akyildiz (2012) employed VOF technique to study the effect of vertical baffle height on sloshing. Cao (2014) studied the sloshing reduction of vertical baffle in rectangular tank based on SPH simulation. In order to reduce sloshing amplitude further and adapt to different situations, many novel and multi baffles were designed. Kim (2001) studied 2-D and 3-D sloshing

in a rectangular tank with a large vertical baffle and three horizontal baffles by using a finite difference method (FDM). Koh et al. (2013) used consistent particle method (CPM) to investigate the effect of a constrained floating baffle in prismatic tank. Xue et al. (2013) conducted experiments to investigate the effects of perforated baffle on the free surface fluctuation and pressure distribution by varying external excitation frequency. Wang et al. (2016) studied the effects of T-shaped baffled parameters on sloshing characteristics in a 2-D elliptical tank by using a semi-analytical scaled boundary finite-element method (SBFEM). Cho and Kim (2016) modeled the dual vertical porous baffles in a swaying rectangular tank to research the effect on reducing sloshing. Yu et al. (2017) arranged two floating vertical baffles near free surface to reduce sloshing pressure by numerical simulation and experiment.

In this paper, an in-house MLParticle-SJTU solver based on improved MPS method is used to simulate 3-D liquid sloshing in rectangular tank. The first section presents some mathematical models of improved MPS. And the liquid sloshing in the tank without baffles is simulated numerically. The results of impact pressure are in good agreement with the experimental data. The nonlinear deformation of free surface can be observed in detail. Then, one vertical baffle is installed in the tank and the position of it from the bottom of tank is changed. The comparison of numerical results shows that different location of vertical baffle affects impact pressure and free surface differently. Considering the variation of filling rate in the using process, the arrangement of multi baffles at different location may be a good method to reduce sloshing amplitude. Finally, two baffles are installed at the bottom of tank and near free surface to study effects on sloshing reduction.

MOVING PARTICLE SEMI-IMPLICIT (MPS) METHOD

Koshizuka and Oka (1996) have explained the MPS method in detail. The flow field is presented by particles which contain the information of mass, velocity, pressure and so on. Therefore, MPS method can simulate violent flow with large deformation and nonlinear fragmentation of free surface effectively (Zhang et al., 2014; Tang et al., 2015-2016; Zhang et al., 2016).

Governing Equations

The governing equations for incompressible and viscous fluid include conservation equations of mass and momentum.

$$\frac{1}{\rho}\frac{D\rho}{Dt} = \nabla \cdot \vec{V} = 0 \tag{1}$$

$$\frac{D\vec{V}}{Dt} = -\frac{1}{\rho}\nabla P + \nu \nabla^2 \vec{V} + \vec{g} \tag{2}$$

where ρ is the fluid density, t is the time, $\vec{V}$ is the velocity vector, P is the pressure, ν is the kinematic viscosity and $\vec{g}$ is the gravitational acceleration vector.

Particle Interaction Models

Kernel Function

A kernel function is used for all interaction models to describe the particle interaction in MPS method.

$$W(r) = \begin{cases} \dfrac{r_e}{0.85r + 0.15r_e} - 1 & 0 \le r < r_e \\ 0 & r_e \le r \end{cases} \tag{3}$$

where r is the distance between two particles and r_e is the radius of the particle interaction. The particle number density and gradient model is $r_e=2.1l_0$, while $r_e=4.0l_0$ is used for the Laplacian model, where l_0 is the initial distance between two adjacent particles.

Gradient Model

The gradient operator is modeled as a local weighted average of the gradient vectors between particle i and its neighboring particle j.

$$<\nabla P>_i = \frac{D}{n^0}\sum_{j\neq i}\frac{P_j + P_i}{|\vec{r}_j - \vec{r}_i|^2}(\vec{r}_j - \vec{r}_i)\cdot W(|\vec{r}_j - \vec{r}_i|) \tag{4}$$

where D is the number of space dimension, n^0 is the initial particle number density and $\vec{r}$ is coordinate vector of fluid particle.

Laplacian Model

The Laplacian operator is modeled by weighted average of the distribution of a quantity ϕ from particle i to its neighboring particle j.

$$<\nabla^2 \phi>_i = \frac{2D}{n^0 \lambda}\sum_{j\neq i}(\phi_j - \phi_i)\cdot W(|\vec{r}_j - \vec{r}_i|) \tag{5}$$

$$\lambda = \frac{\sum_{j\neq i} W(|\vec{r}_j - \vec{r}_i|)\cdot |\vec{r}_j - \vec{r}_i|^2}{\sum_{j\neq i} W(|\vec{r}_j - \vec{r}_i|)} \tag{6}$$

where λ is applied to make sure that the increase of variance is equal to the analytical solution.

Model of Incompressibility

In this paper, the Poisson equation of pressure (PPE) is solved by using a mixed source term method which is developed by Lee et al. (2011).

$$<\nabla^2 P^{k+1}>_i = (1-\gamma)\frac{\rho}{\Delta t}\nabla \cdot \vec{V}_i^* - \gamma \frac{\rho}{\Delta t^2}\frac{<n^*>_i - n^0}{n^0} \tag{7}$$

where γ is a blending parameter which varies from 0 to 1, n^* is the temporal particle number density and Δt is the time step. In this paper, γ=0.01 is employed for all numerical simulations.

Free Surface Detection

Zhang (2012) developed a modified surface particle detection method, which is based on the asymmetry arrangement of neighboring particles.

$$<\vec{F}>_i = \frac{D}{n^0}\sum_{j\neq i}\frac{1}{|\vec{r}_i - \vec{r}_j|}(\vec{r}_i - \vec{r}_j)W(r_{ij}) \tag{8}$$

$$<|\vec{F}|>_i \; > \alpha \tag{9}$$

$$\alpha = 0.9\left|\vec{F}\right|^0 \tag{10}$$

where $\vec{F}$ is a vector which represents the asymmetry of arrangements of neighbor particles, $\left|\vec{F}\right|^0$ is the initial value of $\left|\vec{F}\right|$.

Boundary Condition

In this paper, multilayer particles are used to present the wall boundary. One layer of wall particles is arranged at the boundary. And the pressure of wall particle is solved by PPE. Two layers of ghost particles are configured to fulfill the particle number density near the boundary so that the particle interaction can be properly simulated near the boundary. The pressure of ghost particle is obtained by interpolation.

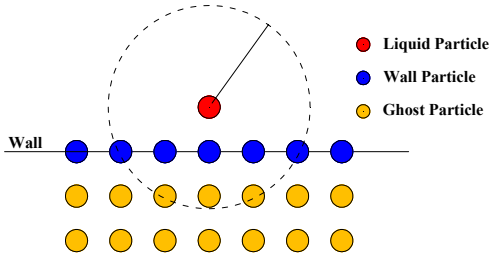

Fig. 1 Schematic of boundary particles

RESULTS AND DISCUSSIONS

Numerical validation

In this section (Case 1), liquid sloshing is simulated in 3-D rectangular tank without baffles under translational excitation. The numerical tank is the same as the experimental model given by Kim (2001). The length (L) of tank is 0.8 m, the width (B) is 0.35 m, the height (H) is 0.5 m and the depth of water (D) is 0.35 m, corresponding filling level is 70%. Fig. 2 shows the sketch of simulated tank. In this paper, all tank models are subject to movement of the external surge excitation:

$$X = A \cdot \sin(\omega \cdot t) \tag{11}$$

where A is the surge amplitude of excitation, ω is the excitation frequency which is $1.1\omega_0$, ω_0 is the lowest natural frequency. The initial particle space is 0.006 m and 584496 particles are used to model. The time step is 5×10^{-4} s and the density of liquid is 1000 kg/m^3. The simulation time is 20 s. It took about 8 days to finish the parallel computation by 10 cores of Intel(R) Xeon(R) E5-2680 v2 2.80GHz. Three pressure probes are fixed on the wall, 0.0525 m, 0.24 m and 0.365 m away from the bottom of tank. Table 1. presents specific locations of pressure probes. Some snapshots of numerical flow field are shown in Figs. 3(a)~(f). In addition, Fig. 4 shows the variation of numerical pressure compared to data of experiment and the spectrum of numerical pressures is shown in Fig. 5.

Table 1. The arrangement of pressure probes in tank

	X	Y	Z
P1	-0.4 m	0 m	0.0525 m
P2	-0.4 m	0 m	0.24 m
P3	-0.4 m	0 m	0.365 m

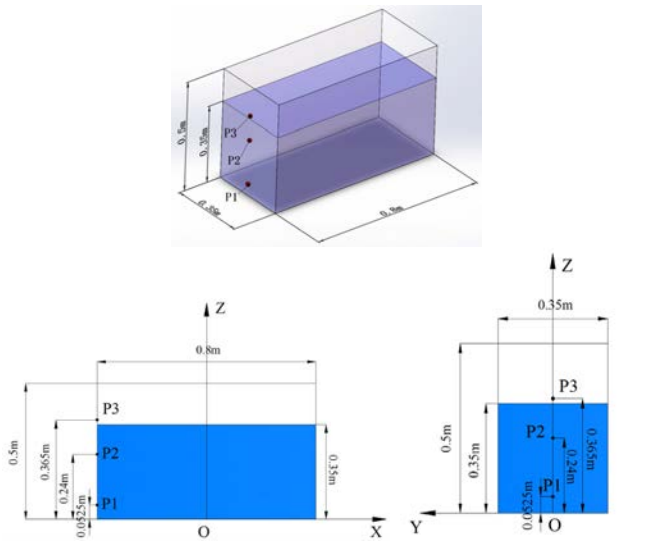

Fig. 2 The sketch of tank

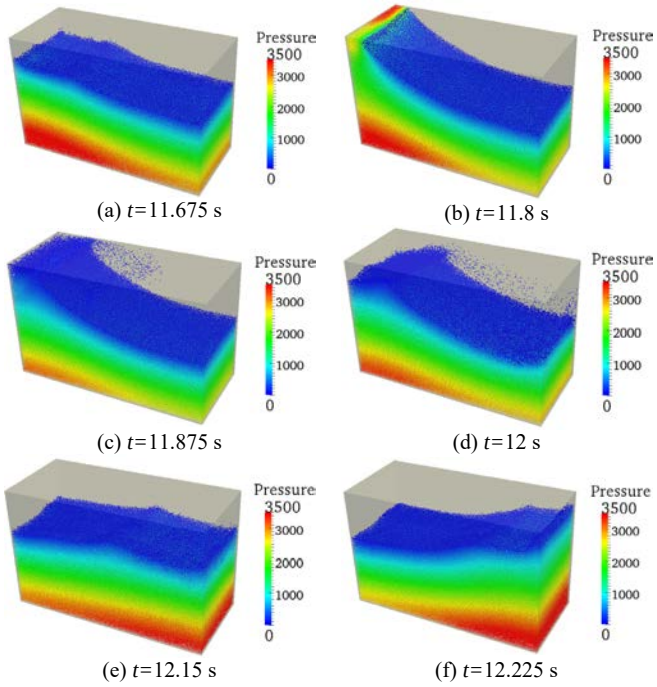

(a) t=11.675 s (b) t=11.8 s

(c) t=11.875 s (d) t=12 s

(e) t=12.15 s (f) t=12.225 s

Fig. 3 The flow field of numerical simulation.

From Fig. 3, many nonlinear deformation and large fragmentation of free surface such as formation of jet, fluid splash and travelling of sloshing wave can be observed clearly. The movement of liquid tank is opposite to the flow of fluid. The fluid flows to the left lateral wall while the tank moves to right. Therefore, the fluid runs up along the lateral wall and lashes the ceiling of tank. Then the head of water spreads along the roof and forms jet. A part of water even splashes on the right side wall. And most overturned fluid still drop down on the free surface under the action of gravity. The left lateral wall pushes fluid to form sloshing wave that transmits to the right side wall.

The pressures of numerical simulation on three probes show a good congruency with results of experiment in Fig. 4. Two successive pressure peaks of P1~P3 in each period can be noticed. Because of the phase difference between fluid and tank, the sloshing wave reaches to and runs up along the lateral wall which results in the increasing impact pressure. Then the fluid that impacts on the ceiling of tank induces the first pressure peak. The second pressure peak results from the fallen water which spreads along the roof and drops down on the free surface. For P3, the phenomenon that water lashes the roof of tank generates the instantaneous pressure peak. In addition, the fallen water results in the fluctuation of pressure. From Fig. 5, the spectrum amplitudes of P1 and P2 are similar to hydrostatic pressure when frequency is 0 Hz. As frequency is the same as excitation frequency ($1.1\omega_0$), there is a peak of spectrum amplitude which is corresponding to the first pressure peak in pressure variation. And another peak of spectrum amplitude illustrated the second pressure peak of each probe when the frequency is twice as excitation frequency.

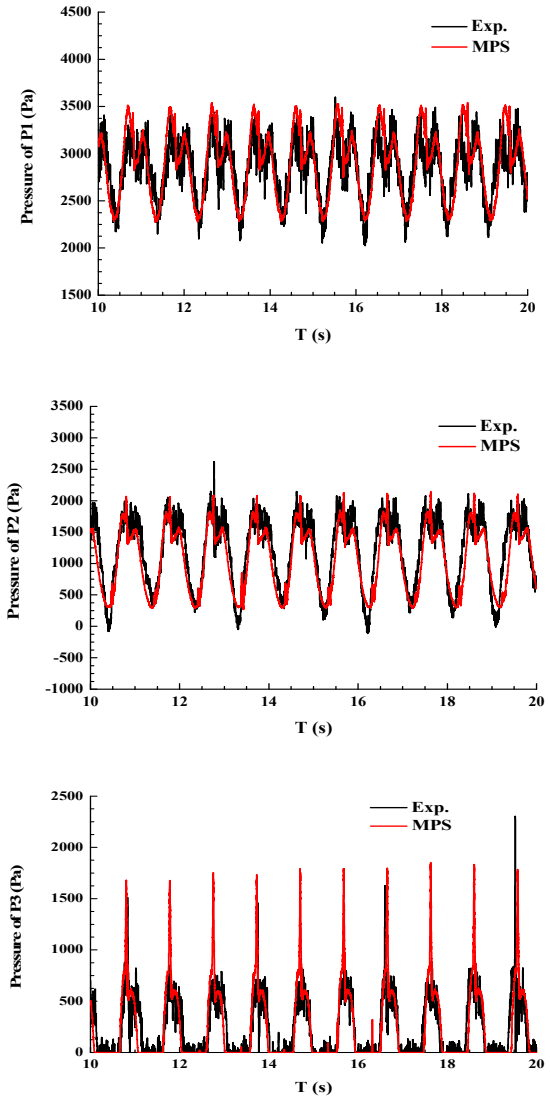

Fig. 4 Comparison of pressures on P1~P3 among experimental and numerical results

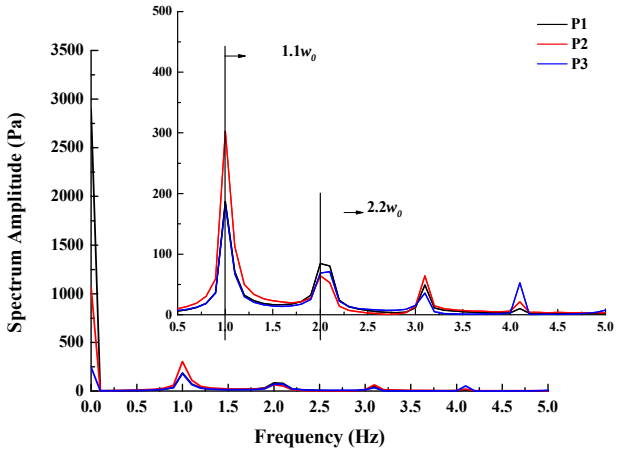

Fig. 5 Spectrum of numerical pressures

Effects of vertical baffles

In this section, one vertical baffle is installed in the middle of tank. The location of baffle is changed to investigate its effects on impact pressure and the deformation of free surface. The baffle is 0.15 m high. And the distance between the center of baffle and the bottom of tank is 0.075 m (Case 2), 0.175 m (Case 3) and 0.275 m (Case 4), respectively. Then, two smaller vertical baffles (Case 5) are installed at the bottom of tank and near free surface. The total height of two baffles is also 0.15 m. The thickness of each baffle is 0.018mm. The 3-D sketches of these four cases are shown in Fig. 6. All cases are also simulated 20 s. It took about 8 days to finish the parallel computation by 10 cores of Intel(R) Xeon(R) E5-2680 v2 2.80GHz.

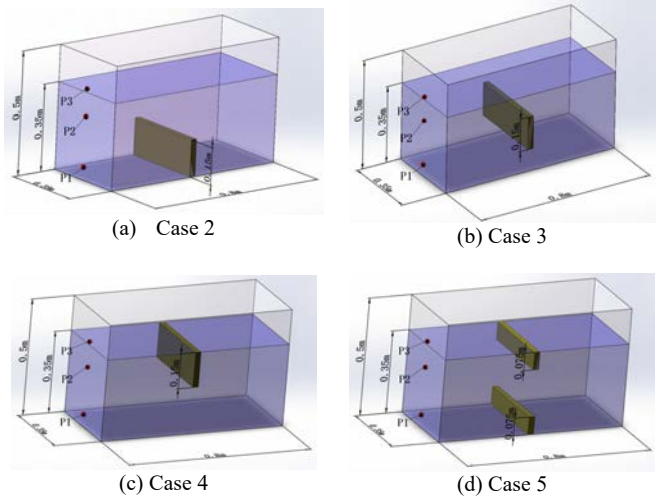

(a) Case 2 (b) Case 3

(c) Case 4 (d) Case 5

Fig. 6 The 3-D sketch of each case

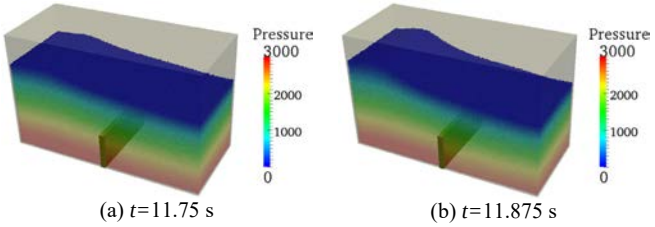

(a) t=11.75 s (b) t=11.875 s

(c) t=11.975 s (d) t=12.125 s

Fig. 7 The snapshots of Case 2

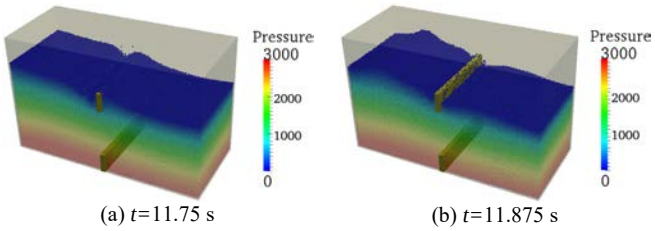

(a) t=11.75 s (b) t=11.875 s

(c) t=11.975 s (d) t=12.125 s

Fig. 10 The snapshots of Case 5

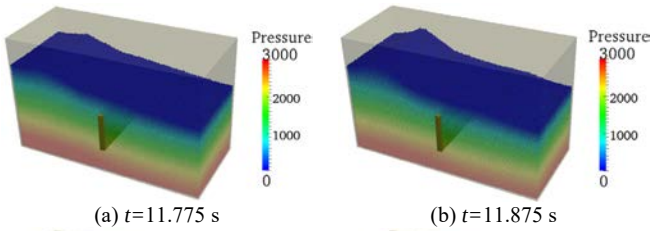

(a) t=11.775 s (b) t=11.875 s

(c) t=11.975 s (d) t=12.125 s

Fig. 8 The snapshots of Case 3

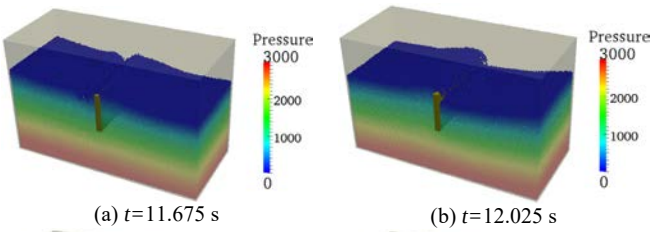

(a) t=11.675 s (b) t=12.025 s

(c) t=12.2 s (d) t=12.325 s

Fig. 9 The snapshots of Case 4

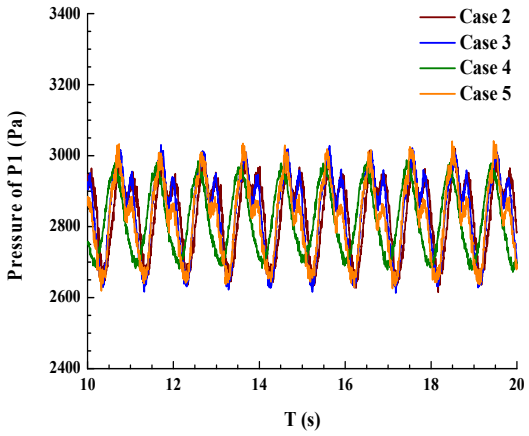

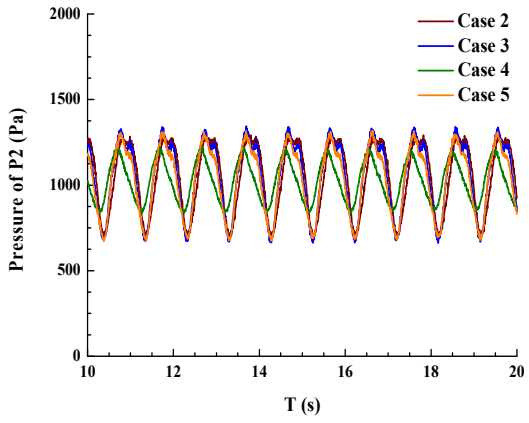

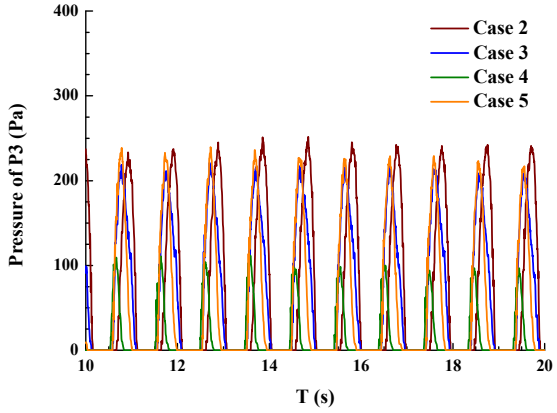

Fig. 11 The time history of dynamic pressure on P1~P3

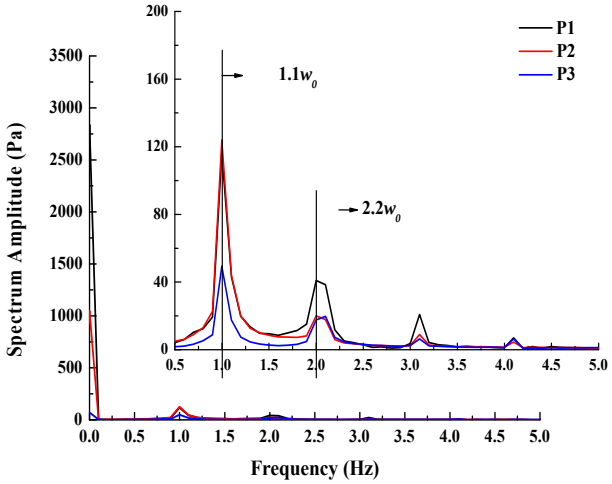

Fig. 12 Spectrum of numerical pressures for case 2

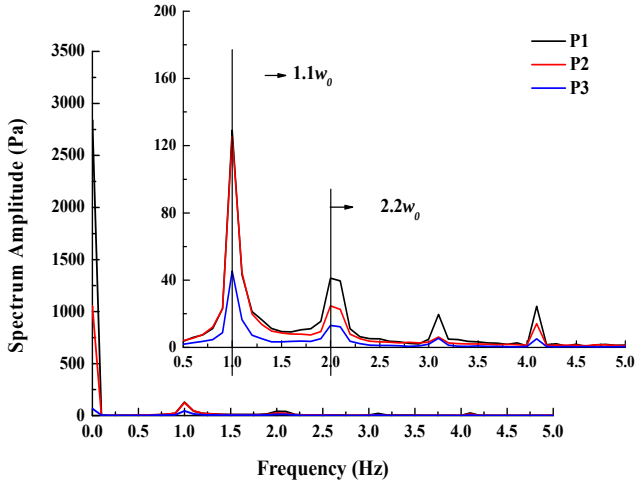

Fig. 13 Spectrum of numerical pressures for case 3

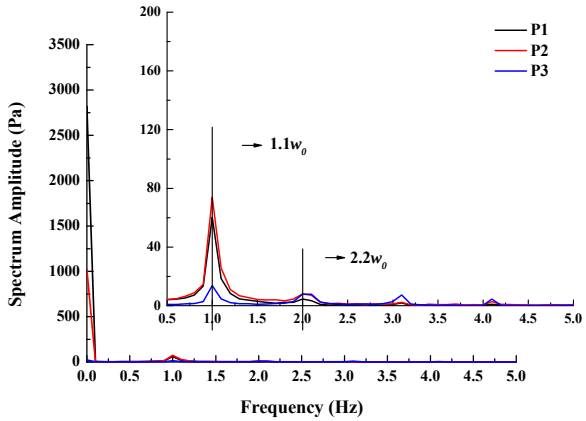

Fig. 14 Spectrum of numerical pressures for case 4

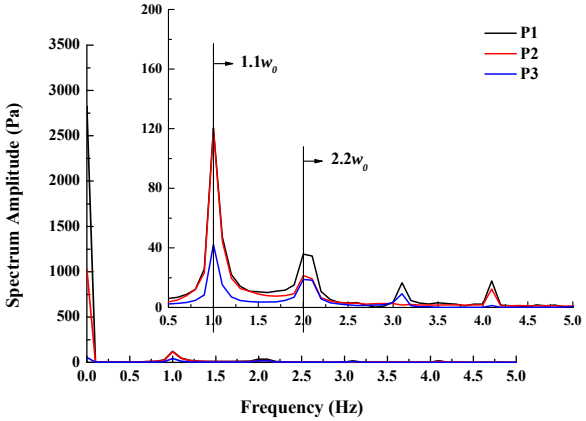

Fig. 15 Spectrum of numerical pressures for case 5

Some instants of fluid field are presented in Figs. 7~10 for different cases. Comparing to Case 1, many nonlinear phenomena of free surface has been disappeared because of the vertical baffles. In Case 2, when the liquid tank moves to right side, the left wall pushes water. But the fluid still flows to the left wall at this time. The phase difference of movements between fluid and tank generates an embossment of free surface near left side wall. In the whole process of sloshing, the sloshing wave can be observed clearly. And the free surface of Case 2 is smoother than Case1. In Case 3, the fluctuation of free surface is obviously larger than Case 2. A higher peak of free surface forms when the fluid flows over the vertical baffle in Fig. 8(d). It is similar to the situation when wave travels from deep water to shallow. Therefore, in Fig. 8(a) the embossment of free surface near side wall is sharper than Case 2. In addition, the bottom pressure field is more continuous in Case 3. In Case 4, the free surface is divided into two components whose movements are almost synchronous. From Fig. 9, the left part of free surface overturns when the fluid flows over the baffle. Then the overflowed fluid falls into the right fluid field and forms a hollow on free surface. The vertical baffle of Case 4 is more effective to restrain the free surface. And the height of water that runs along lateral wall is shorter than Case 2 and 3. In Case 5, the deformation of free surface is larger than that of Case 4. The fluid fiercely slaps the baffle near free surface. And some particles splash in this process which embodies the characteristic of Lagrangian method. An obvious embossment of free

surface can be observed in Fig. 10(b) which is similar to Case 3. Furthermore, the bottom baffle restrains the flow of lower fluid. The fluid field of Case 5 has all characteristics of Case 2~4.

Fig. 11 shows the variation of pressure with time on P1~P3. Obviously, the pressures of all cases with baffles are much smaller than Case 1. And different arrangements of vertical baffles affect the characteristics of pressure. The pressures of P1 and P2 still appear two successive peaks in Case 2, 3 and 5. When the sloshing wave travels and impacts the side wall, the first pressure peak occurs. And the second pressure peak result from the embossment of free surface mentioned before. When the fallen water travels to right side wall, the vertical baffle obstructs this movement. The pressure of Case 4 is sinusoidal and smaller than other cases. The vertical baffle near free surface is effective to restrain the flow of free surface and water running up along lateral wall. Therefore, Case 4 is the best arrangement of baffle to reduce the impact pressure of sloshing. The baffle arrangement of Case 5 can also reduce impact pressure. Because of the shorter baffle at the bottom, the block function plays a less role in mitigating the free surface. Therefore, the second pressure peaks of Case 5 on P1 and P2 are smaller than Case 2 and 3.

The spectrums of numerical pressures on P1~P3 for each case are shown in Fig. 12~15. As frequency is 0 Hz, the spectrum amplitudes of P1 and P2 are similar to hydrostatic pressure. For case 2, 3 and 5, there are two peaks of spectrum amplitude when frequency is $1.1\omega_0$ and $2.2\omega_0$. These two peaks can explain the appearance of two successive peaks for P1 and P2. But as frequency is $2.2\omega_0$, the spectrum amplitude is so small that only one pressure peak can be observed obviously in pressure variation for case 4 and P3 of each case.

CONCLUSIONS

In this paper, MLParticle-SJTU solver based on improved MPS method is used to investigate the effects of arrangement of vertical baffles on 3-D liquid sloshing under horizontal excitation. Based on the results of numerical simulation, the following conclusions can be drawn:

(1) The impact pressures of numerical simulation in liquid tank without baffles shows a good agreement with the experimental data, which demonstrates the validity of MLParticle-SJTU solver. The typical two successive pressure peaks in each period can be noticed. And large deformation and nonlinear fragmentation of free surface, like hitting the roof, formation of jet, fluid splash and so on, can be observed clearly in numerical simulation.

(2) All arrangements of vertical baffles can effectively reduce the amplitude of sloshing. Different arrangements have different effects on fluid field and impact pressure. And the vertical baffle installed near free surface is the most effective scheme to reduce impact pressure.

(3) Two vertical baffles are also effective arrangement to reduce the sloshing amplitude. The fluid field and impact pressure possess characteristics of other cases. Considering different filling rate in the reality (not only high filling rater in this paper), multi baffles installed at different location of tank may be a better method to reduce sloshing in complex conditions. The effects of multi baffles will be more researched in the future.

ACKNOWLEDGEMENTS

This work is supported by the National Natural Science Foundation of China (51379125, 51490675, 11432009, 51579145), Chang Jiang Scholars Program (T2014099), Shanghai Excellent Academic Leaders Program (17XD1402300), Shanghai Key Laboratory of Marine Engineering (K2015-11), Program for Professor of Special Appointment (Eastern Scholar) at Shanghai Institutions of Higher Learning (2013022), Innovative Special Project of Numerical Tank of Ministry of Industry and Information Technology of China (2016-23/09) and Lloyd's Register Foundation for doctoral student, to which the authors are most grateful.

REFERENCES

Akyildiz, H (2012). "A Numerical Study of the Effects of the Vertical Baffle on Liquid Sloshing in Two-dimensional Rectangular Tank," *Journal of Sound and Vibration*, 331, 41-52.

Arai, M, Cheng, LY, and Inoue, Y (1992). "3D Numerical Simulation of Impact Load due to Liquid Cargo Sloshing," *Journal of the Society of Naval Architects of Japan*, 171, 177-184.

Bulian, G, Botiavera, B, and Soutoiglesias, A (2014). "Experimental Sloshing Pressure Impacts in Ensemble Domain: Transient and Stationary Statistical Characteristics," *Physics of Fluid*, 2014, 26 (3), 132-143.

Cao, XY, Ming, FR, and Zhang, AM (2014). "Sloshing in a Rectangular Tank Based on SPH Simulation," *Applied Ocean Research*, 47, 241-254.

Cho, IH, and Kim, MH (2016). "Effect of Dual Vertical Porous Baffles on Sloshing Reduction in a Swaying Rectangular Tank," *Ocean Engineering*, 126, 364-373.

Delorme, L, Colagrossi, A, Iglesias, AS, Rodriguez, RZ, and Vera, EB (2009). "A Set of Canonical Problems in Sloshing, Part I: Pressure Field in Forced Roll-comparison between Experimental Results and SPH," *Ocean Engineering*, 36 (2), 168-178.

Faltinsen, OM (1978). "A Numerical Nonlinear Method of Sloshing in Tanks with Two Dimensional Flow," *Journal of Ship Research*, 22 (3), 193-202.

Faltinsen, OM, Rognebakke, OF, Lukovsky, JA, and Timokha, AM (2000). "Multidimensional modal analysis of non-linear sloshing in a rectangular tank with finite water depth," *Journal of Fluid Mechanics*, 407, 201-234.

Kim, Y (2001). "Numerical Simulation of Sloshing Flow with Impact Load," *Applied Ocean Research*, 23, 53-62.

Koh, CG, Luo, M, and Bai, W (2013). "Modelling of Liquid Sloshing with Constrained Floating Baffle," *Computers and Structures*, 122, 270-279.

Koh, HM, Kim, JK, and Park, JH (1998). "Fluid-structure Interaction Analysis of 3-D Rectangular Tanks by a Variationally Coupled BEM-FEM and Comparison with Test Eesults," *Earthquake Engineering and Structural Dynamics*, 27 (27), 109-124.

Koshizuka, S, and Oka, Y (1996). "Moving-particle Semi-implicit Method for Fragmentation of Incompressible Fluid," *Nuclear Science and Engineering*, 123 (3), 421-434.

Lee, BH, Park, JC, Kim, MH, and Hwang, SC (2011). "Step-by-step Improvement of MPS Method in Simulating Violent Free-surface Motions and Impact-loads," *Computer Methods in Applied Mechanics and Engineering*, 200 (9-12), 1113-1125.

Liu, DM, and Lin, PZ (2008). "A numerical study of three-dimensional liquid sloshing in tanks," *Journal of Computational Physics*, 227, 3921-3939.

Liu, DM, and Lin, PZ (2009). "Three-dimensional Liquid Sloshing in a Tank with Baffles," *Ocean Engineering*, 36, 202-212.

Nakayama, T, and Washizu, K (1980). "Nonlinear Analysis of Liquid Motion in a Container Subjected to Forced Pitching Oscillation," *International Journal for Numerical Methods in Engineering*, 15 (8), 1207-1220.

Nakayama, T, and Washizu, K (1981). "The Boundary Element

Method Applied to the Analysis of Two-dimensional Nonlinear Sloshing Problems," *International Journal for Numerical Methods in Engineering*, 17 (11), 1631-1646.

Park, JJ, Kim, SY, Kim, Y, Seo, JH, Jin, CH, Joh, KH, Kim, BW, and Suh, YS (2015). "Study on Tank Shape for Sloshing Assessment of LNG Vessels under Unrestricted Filling Operation," *Journal of Marine Science & Technology*, 1-12.

Wu, GX, Ma, QW, and Taylor, RE (1998). "Numerical Simulation of Sloshing Waves in a 3D Tank Based on a Finite Element Method," *Applied Ocean Research*, 20 (6), 337-355.

Shao, JR, Li, HQ, Liu, GR, and Liu, MB (2012). "An Improved SPH Method for Modeling Liquid Sloshing Dynamics," *Computers and Structures*, 100-101, 18-26.

Souto-Iglesias, A, Bulian, G, and Botia-Vera, E (2015). "A Set of Canonical Problems in Sloshing. Part 2: Influence of Tank Width on Impact Pressure Statistics in Regular Forced Angular Motion," *Ocean Engineering*, 105, 136-159.

Tang, ZY, and Wan, DC (2015). "Numerical Simulation of Impinging Jet Flows by Modified MPS Method," *Engineering Computations*, 32(4), 1153-1171.

Tang, ZY, Zhang, YL, and Wan, DC (2016). "Numerical Simulation of 3D Free Surface Flows by Overlapping MPS," *Journal of Hydrodynamics*, 28(2), 306-312.

Tang, ZY, Zhang, YL, and Wan, DC (2016). "Multi-Resolution MPS Method for Free Surface Flows," *International Journal of Computational Methods*, 13(4), 1641018-1-1641018-17.

Wang, WY, Guo, ZJ, Peng, Y, and Zhang, Q (2016). "A Numerical Study of the Effects of the T-shaped Baffles on Liquid Sloshing in Horizontal Elliptical Tanks," *Ocean Engineering*, 111, 543-568.

Xue, MA, Zheng, JH, Lin, PZ, Ma, Y, and Yuan, XL (2013). "Experimental Investigation on the Layered Liquid Sloshing in a Rectangular Tank," *Proceedings of the Twenty-third (2013) International Offshore and Polar Engineering*, Anchorage, Alaska, USA, ISOPE, (3) 202-208.

Xue, MA, Lin, PZ, Zheng JH, Ma YX, Yuan XL, and Nguyen, VT (2013). "Effects of Perforated Baffle on Reducing Sloshing in Rectangular Tank: Experimental and Numerical Study," *Chinese Ocean Engineering*, 27 (5), 615-628.

Yang, YQ, Tang, ZY, Zhang, YL, and Wan, DC (2015). "Investigation of Excitation Period Effects on 2D Liquid Sloshing by MPS Method," *Proceedings of the Twenty-fifth (2015) International Ocean and Polar Engineering Conf*, Hawaii, ISOPE, (3) 937-944.

Yu, YM, Ma, N, Fan, SM, and Gu, XC (2017). "Experimental and Numerical Studies on Sloshing in a Membrane-type LNG Tank with Two Floating Plates," *Ocean Engineering*, 129, 217-227.

Zhang, YL, Tang, ZY, and Wan, DC (2016). "Numerical Investigations of Waves Interacting with Free Rolling Body by Modified MPS Method," *International Journal of Computational Methods*, 13(4), 1641013-1-1641013-14.

Zhang, YX, and Wan, DC (2012). "Numerical simulation of liquid sloshing in low-filling tank by MPS," *Journal of Hydrodynamics*, 27 (1), 101-107.

Zhang, YX, and Wan, DC (2014). "Comparative Study of MPS Method and Level-set Method for Sloshing Flows," *Journal of Hydrodynamics*, 26 (4), 577-585.